Spatial distribution of protein molecules adsorbed at a polyelectrolyte multilayer

Guido Jackler and Claus Czeslik*
Universität Dortmund, Physikalische Chemie I, D-44221 Dortmund, Germany

Roland Steitz
Hahn-Meitner-Institut, D-14109 Berlin, Germany

Catherine A. Royer
Centre de Biochimie Structurale, INSERM, F-34090 Montpellier, France
(Received 9 September 2004; published 27 April 2005)

The spatial distribution of protein molecules interacting with a planar polyelectrolyte multilayer was determined using neutron reflectometry. Staphylococcal nuclease (SNase) was used as model protein that was adsorbed to the multilayer at 22 °C and 42 °C. At each temperature, the protein solution was adjusted to *p*D-values of 4.9 and 7.5 to vary the net charge of the protein molecules. The multilayer was built up on a silicon wafer by the deposition of poly(ethylene imine) (PEI), poly(styrene sulfonate) (PSS), and poly(allylamine hydrochloride) (PAH) in the order Si-PEI-PSS-$(PAH\text{-}PSS)_5$. Applying the contrast variation technique, two different neutron reflectivity curves were measured at each condition of temperature and *p*D-value. From the analysis of the curves, protein density profiles normal to the interface were recovered. Remarkably, it has been found that SNase is partially penetrating into the polyelectrolyte multilayer after adsorption at all conditions studied. The measured neutron reflectivities are consistent with a penetration depth of 50 Å at *p*D=4.9 and 25 Å at *p*D=7.5. Since SNase has an isoelectric point of *p*H=9.5, it carries a net positive charge at both *p*D-values and interacts with the PSS final layer under electrostatic attraction conditions. However, when increasing the temperature, the amount of adsorbed protein is increasing at both *p*D-values indicating the dominance of entropic driving forces for the protein adsorption. Interestingly, at *p*D=4.9 where the protein charge is relatively high, this temperature-induced mass increase of immobilized protein is more pronounced within the polyelectrolyte multilayer, whereas at *p*D=7.5, closer to the isoelectric point of SNase, raising the temperature has mainly the effect to accumulate protein molecules outside the polyelectrolyte multilayer at the water interface. It is suggested that the penetration of SNase into the polyelectrolyte multilayer is related to a complexation mechanism. The complexation is essentially entropic in nature due to the release of counterions.

DOI: 10.1103/PhysRevE.71.041912 PACS number(s): 87.68.+z, 68.35.Ct

I. INTRODUCTION

The immobilization of proteins at interfaces plays a key role in a series of biomedical and biotechnological processes [1,2]. For example, contact of blood with artificial implants may be followed by the adsorption of adhesion proteins such as fibrinogen which can initiate platelet adhesion and blood coagulation. Solid-phase immunoassays rely on the immobilization of antibody molecules on a sorbent surface to capture an antigen, whereas bovine serum albumin may be adsorbed to free sorbent surface areas to prevent unspecific binding reactions. Furthermore, protein biochips are of increasing importance in proteomics where proteins are identified and characterized in terms of protein interactions by their binding to a large number of chemically modified small spots.

Since protein molecules are only marginally stable, interactions with interfaces can induce unfavorable changes in their conformation and dynamics [3–7]. As a consequence, their biological activity and function will be reduced drastically. Thus, there is an intense research effort to develop surface coatings that provide a mild protein environment for a controlled protein immobilization without denaturation. In a promising approach, polyelectrolyte molecules are grafted to a materials surface to form a so-called polyelectrolyte brush. These polyelectrolyte brushes represent a unique surface coating for protein immobilization, since their protein binding capacity can be "switched" by the ionic strength of the protein solution independent of the protein net charge [8–10]. Moreover, it could be shown that the secondary structure and the enzymatic activity of several proteins are preserved at these brushes [11,12]. Alternatively, materials surfaces can be modified with a so-called polyelectrolyte multilayer. Applying the layer-by-layer deposition technique, these multilayers are built up by the consecutive adsorption of positively and negatively charged polyelectrolytes on a planar solid substrate [13,14].

Over the past years, the formation of polyelectrolyte multilayers and their interaction with proteins have been studied extensively [15–18]. It has been established that proteins can be adsorbed to or embedded within the multilayers thereby preserving their native conformation and biological activity to a large extent [19–25]. However, there is still a lack of knowledge about the kind of interactions between protein molecules and the polyelectrolyte multilayers. There are good reasons to assume that these interactions are mainly of

*Author to whom correspondence should be addressed.

electrostatic origin [26,27]. On the other hand, it is reported that a polyelectrolyte-protein association is entropically driven by a release of counterions [28]. Furthermore, it is widely unknown how protein molecules which are adsorbed to a polyelectrolyte multilayer arrange at the interface. It is generally assumed that the protein adsorbate simply forms an additional layer on top of the polyelectrolyte multilayer. However, as has been reported recently, positively charged colloidal beads penetrate deeply into a polyelectrolyte multilayer composed of poly(styrene sulfonate) (PSS) and poly(allylamine hydrochloride) (PAH) [29]. Thus, one may speculate that protein molecules adsorbing to a polyelectrolyte multilayer do not simply form an additional layer but may partially be incorporated into the outer region of the polyelectrolyte multilayer. Indeed, it has already been discussed that protein molecules adsorbed on a polyelectrolyte multilayer may partially be covered by diffusing polyelectrolyte chains [23,27].

In this study, we have determined the density profile of a protein adsorbate interacting with a polyelectrolyte multilayer by using neutron reflectometry. The main aim was to find out, if the adsorbed protein penetrates into the multilayer. The multilayer was deposited on a planar silicon (Si) wafer and was composed of the polyelectrolytes poly(ethylene imine) (PEI), PSS and PAH in the order Si-PEI-PSS-$(PAH\text{-}PSS)_5$ where PSS forms the final layer. Staphylococcal nuclease (SNase) was used as model protein which consists of 149 amino acid residues and is characterized by an isoelectric point of about 9.5. Thus, at the *p*D-values used in this study, it carries a net positive charge and is interacting with the PSS final layer under electrostatic attraction conditions. Neutron reflectometry is the most powerful tool to determine the structure of a solid/aqueous interface that is interacting with protein molecules, since neutrons can penetrate condensed matter over macroscopic distances, contrast variation is easily achieved, and interfacial structures can be resolved with Å resolution [30]. As will be shown here, the adsorption of SNase does not lead to a simple adsorbate layer on top of the polyelectrolyte multilayer, but to a partial penetration of SNase into the PSS-PAH multilayer. Furthermore, by changing the temperature and the *p*D-value of the samples, the type of protein-polyelectrolyte interactions was characterized. From the protein density profiles obtained under the various conditions, one may conclude that the penetration of the protein into the polyelectrolyte multilayer is related to a complexation mechanism associated with a release of counterions. Since the biological activity of enzyme molecules adsorbed at a polyelectrolyte multilayer depends on the accessibility of the enzyme by the substrate, the experimental findings presented in this study may help to understand this biological activity in a better way.

II. EXPERIMENT

SNase was obtained as described before [31]. It was analyzed by gel electrophoresis and was found to be essentially pure ($>99\%$). A sodium phosphate buffer solution was prepared in D_2O with a concentration of 10 mM and a *p*D-value of 7.5. For a lower *p*D-value of 4.9, a sodium acetate buffer solution was used instead that was adjusted with hydrochloric acid. Final sample solutions were prepared with an SNase concentration of 0.05 mg/ml in D_2O buffer solution. For contrast variation experiments, a mixture of D_2O and H_2O buffer solutions with a volume ratio of 3:1 was chosen which will be denoted as HDO in the following. Si wafers were purchased from Siliciumbearbeitung Andrea Holm (Tann, Germany). They had a size of 8 cm $\times$ 5 cm $\times$ 1.5 cm, with the two large sides being polished. The wafers were cleaned by heating them in a mixture of 30 ml hydrogen peroxide (30%) and 70 ml sulfuric acid (97%) followed by intensive rinsing with pure water. The polyelectrolytes PEI ($M_w = 750\,000$ g mol^{-1}), PSS ($M_w = 70\,000$ g mol^{-1}) and PAH ($M_w = 70\,000$ g mol^{-1}) were obtained from Sigma (Steinheim, Germany) and used as supplied. A polyelectrolyte multilayer was built up on an Si wafer by an initial immersion of the wafer into a PEI aqueous solution (0.01 mol/l monomers) for 20 min. The wafer was then alternately immersed into PSS and PAH aqueous solutions (0.01 mol/l monomers, 1 mol/l sodium chloride) for 20 min in each case. After each polyelectrolyte deposition step, the Si wafer was rinsed intensively with pure water. Finally, an Si wafer with the structure Si-PEI-PSS-$(PAH\text{-}PSS)_5$ was heated in a water bath to 55 °C for about 6 h and dried at the air. By this heat treatment, the polyelectrolyte multilayer is annealed to prevent structural changes when heating the multilayer from 22 to 42 °C during the experiments.

The neutron reflectivity measurements were performed at the Hahn-Meitner-Institut in Berlin (Germany) using the instrument V6 [32] The neutron wavelength selected by a graphite monochromator was 4.66 Å; higher-order wavelengths were suppressed by a Be filter cooled with liquid nitrogen. The sample cell consisted of an Si wafer coated with a polyelectrolyte multilayer at the bottom surface (8 cm $\times$ 5 cm) and a Teflon trough, which was fixed to the bottom surface of the Si wafer and was filled with the sample solution. The sample cell was heated using a thermostating water jacket. The neutrons entered the Si wafer through one of the small sides, were reflected in part at the Si-solution interface, and left the Si wafer through the other small side. Neutron reflectivities were recorded with a fixed incident neutron beam in $\theta/2\theta$ geometry using a ^{3}He detector. Raw data were normalized to the number of incoming neutrons hitting the Si-solution interface and scaled as a function of momentum transfer, $Q = (4\pi/\lambda)\sin\theta$ (λ is the neutron wavelength and θ is the angle of incidence). θ ranges from 0° to about 2.5°. Prior to each run, the sample cell was rinsed and filled with freshly prepared sample solution and was equilibrated for at least 1 h.

III. DATA ANALYSIS

The measured neutron reflectivity curves were analyzed by fitting calculated curves to the measured curves. Calculations were performed on the basis of the optical matrix method where the interfacial structure is decomposed into layers [33]. Each layer is characterized by the scattering length density ρ and the layer thickness d. In addition, the interface between two layers is described by the roughness

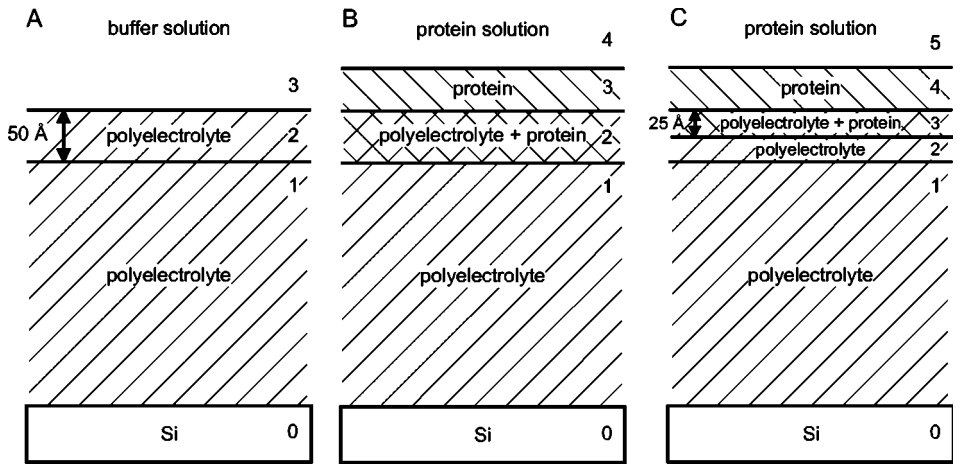

FIG. 1. Schematic representation of the interfacial structure model used to analyze the measured neutron reflectivity data. (A) Structure in the absence of protein. An upper polyelectrolyte layer of 50 Å thickness is assumed into which protein molecules can penetrate after adsorption. (B) Structure in the presence of proteins. Protein molecules are incorporated into the upper polyelectrolyte layer and form an additional adsorbate layer. (C) Protein molecules are allowed to penetrate into the upper 25 Å of the polyelectrolyte multilayer only.

σ. Fitting parameters are thus the scattering length densities and layer thicknesses of each layer, the interlayer roughnesses, and the scattering length densities of the first and the last semi-infinite layers (Si wafer and sample solution). The deviation between the measured and the calculated neutron reflectivity curve was quantified as

$$\chi^2 = \frac{1}{n}\sum_i \left(\frac{R_{i,\mathrm{meas}} - R_{i,\mathrm{cal}}}{R_{i,\mathrm{meas}}} \right)^2, \qquad (1)$$

where n is the total number of data points, $R_{i,\mathrm{meas}}$ and $R_{i,\mathrm{cal}}$ are the measured and calculated reflectivities of data point i, respectively. As mentioned in the Experiment, contrast variation was performed for each sample. The two neutron reflectivity curves thus obtained were analyzed globally by linking the layer thicknesses and the interlayer roughnesses across the pair of curves. This global analysis largely reduces the number of scattering length density profiles consistent with the experimental data. Furthermore, the scattering length densities of the Si wafer and the sample solutions were not varied in the fitting procedure. They were fixed to values of $2.07 \cdot 10^{-6}$ Å^{-2} (Si), $6.37 \cdot 10^{-6}$ Å^{-2} (D_2O as solvent) and $4.64 \cdot 10^{-6}$ Å^{-2} (HDO as solvent) [34]. It should be noted that the scattering length density of each intermediate layer containing various amounts of polyelectrolyte, protein and buffer solution was not used as direct fitting parameter but decomposed according to

$$\rho_i = \rho_{\mathrm{pol}}\phi_{\mathrm{pol},i} + \rho_{\mathrm{pro}}\phi_{\mathrm{pro},i} + \rho_{\mathrm{sol}}(1 - \phi_{\mathrm{pol},i} - \phi_{\mathrm{pro},i}), \qquad (2)$$

where ρ_{pol} is the scattering length density of the pure polyelectrolyte (fitting parameter), ρ_{pro} is that of the pure protein (fixed parameter), and ρ_{sol} is that of the sample solution (fixed parameter). $\phi_{\mathrm{pol},i}$ and $\phi_{\mathrm{pro},i}$ are the volume fractions of polyelectrolyte and protein in layer i (fitting parameters). The scattering length density of SNase was calculated from its sum formula and volume. Values of $3.15 \cdot 10^{-6}$ Å^{-2} (in D_2O at 22 °C), $3.12 \cdot 10^{-6}$ Å^{-2} (in D_2O at 42 °C), $2.80 \cdot 10^{-6}$ Å^{-2} (in HDO at 22 °C), and $2.77 \cdot 10^{-6}$ Å^{-2} (in HDO at 42 °C) were obtained and used in the analysis. The volume of SNase is 21 100 Å^3 at 22 °C and 21 300 Å^3 at 42 °C which was determined by density measurements [35]. The hydrating water molecules of the protein have been treated as part of the whole water volume fraction, i.e., they are modeled using the scattering length density ρ_{sol}.

To describe the polyelectrolyte multilayer in contact with buffer solution without protein, a two-layer model was chosen [Fig. 1(a)]. The first layer (index 1) represents the lower main part of the polyelectrolyte multilayer in contact with the Si wafer, whereas the second layer (index 2) extends over the upper 50 Å of the polyelectrolyte multilayer. This second layer is introduced, because it is assumed in the following that protein molecules can partially penetrate into it. As will be shown below, the polyelectrolyte multilayers studied here have a thickness of about 310 Å. Thus, each of the 12 deposited polyelectrolyte layers is about 26 Å thick. However, since the polyelectrolyte layers partially overlap, the concentration profile of a single layer has a full width at half height that is twice this value (about 52 Å) [13]. It is believed that SNase only interacts strongly with the final PSS layer under electrostatic attraction conditions. Thus, it is very important to model precisely the scattering length density of the upper 50 Å of the polyelectrolyte multilayer in the absence of protein. The change of this scattering length density in the presence of protein is then a measure for the volume fraction of protein inside the polyelectrolyte multilayer. In the presence of protein, the structure model described above is extended with an additional layer to account for the protein adsorbate [Figs. 1(b) and 1(c)]. Protein may also be incorporated into the upper 50 Å of the polyelectrolyte multilayer [Fig. 1(b)]. In addition, it has also been tested, if the protein is present in the upper 25 Å of the polyelectrolyte multilayer only [Fig. 1(c)]. Thus, by choosing the two penetration depths of 50 and 25 Å one can probe the tendency for protein incorporation. Of course, these two penetration depths represent test parameters.

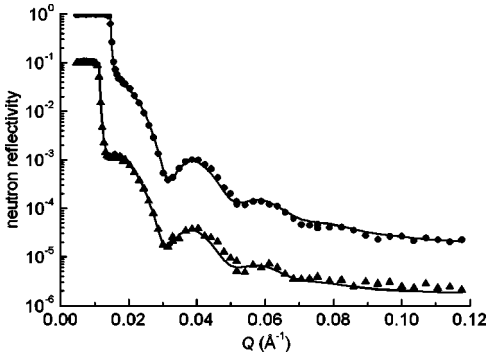

FIG. 2. Neutron reflectivity curves of a polyelectrolyte multilayer at the interface between a Si wafer and a buffer solution without protein (pD=7.5, T=22 °C). The symbols represent the experimental data with D_2O as the solvent (circles) and HDO as the solvent (triangles, shifted by 0.1 on the reflectivity axis), whereas the solid lines show a global fit to both curves.

IV. RESULTS AND DISCUSSION

In Fig. 2, neutron reflectivity curves are shown that were obtained for an Si-PEI-PSS-(PAH-PSS)$_5$-buffer solution interface in the absence of SNase (pD=7.5, 22 °C). The two curves measured with D_2O and HDO as the solvent were analyzed globally using the structure model shown in Fig. 1(a). The fitting results are summarized in Table I and corresponding calculated neutron reflectivity curves are shown in Fig. 2 as solid lines. Table I also includes data of a second polyelectrolyte multilayer that was prepared in the same way but characterized at a lower pD-value of 4.9. As can be seen from Table I, the structures of both polyelectrolyte multilayers are almost identical. Apparently, the pD-value does not influence the polyelectrolyte multilayer structure. At both pD-values, the volume fraction of the polyelectrolyte is about 0.53 and its scattering length density is found to be about $2.3 \cdot 10^{-6}$ Å^{-2} in good agreement with values reported in other studies [15,36]. The small increase of ϕ_{pol} observed at pD=7.5 just below the polyelectrolyte-solution interface (Table I) is believed to be a result of the drying of the hot wafer after heat treatment (see experimental section). However, an increased pD-value of 7.5 could lead to a slightly less dense packing of the polyelectrolyte associated with an increased polyelectrolyte volume fraction. It is noted that the relatively large roughness σ_{01} is used to model the transition from the Si wafer to the first PSS layer thereby covering the thin silicon oxide film and the initial PEI layer.

TABLE I. Structure of an Si-PEI-PSS-(PAH-PSS)$_5$-buffer solution interface.[a]

pD	d_1 (Å)	d_2 (Å)	ρ_{pol} (Å^{-2})	$\phi_{\mathrm{pol},1}$	$\phi_{\mathrm{pol},2}$
4.9	262	50	2.26×10^{-6}	0.53	0.50
7.5	260	50	2.32×10^{-6}	0.53	0.61

[a]For each pD-value, a different Si wafer was used. The structure model shown in Fig. 1(a) was assumed. d_2 was not varied. ρ_{pol} is given for D_2O as solvent. Interlayer roughnesses are found to be σ_{01}=31 Å, σ_{12}=5 Å, σ_{23}=3 Å.

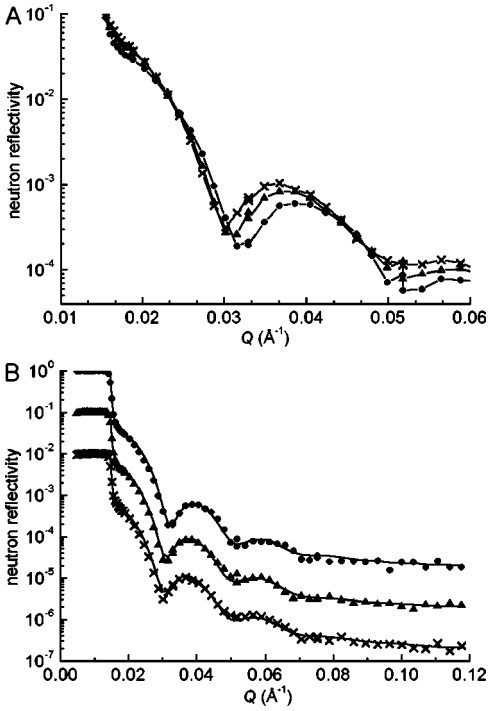

FIG. 3. Neutron reflectivity curves of a Si-PEI-PSS-(PAH-PSS)$_5$-solution interface with D_2O as the solvent at pD=4.9. In (A), measured reflectivities are shown over a limited Q-range to illustrate the changes when SNase binds to the polyelectrolyte multilayer at different temperatures. Data are given for the buffer solution at 22 °C (circles), the buffer solution containing 0.05 mg/mL SNase at 22 °C (triangles), and the buffer solution containing 0.05 mg/mL SNase at 42 °C (crosses). In (B), the same measured data are shown as symbols together with fitted neutron reflectivity curves represented as solid lines. Data in (B) are shifted on the reflectivity axis for clarity.

In Fig. 3, selected neutron reflectivity curves of an Si-PEI-PSS-(PAH-PSS)$_5$-buffer solution interface are shown before and after the addition of 0.05 mg/ml SNase (D_2O as solvent, pD=4.9). Similar data were obtained at pD=7.5. From the curves shown in Fig. 3(a), it is clear that SNase binds to the polyelectrolyte multilayer, since the oscillation observed in the Q-range of 0.03–0.05 Å^{-1} is shifting to smaller Q-values when SNase is added to the buffer solution at 22 °C. This shift is even more pronounced when the temperature is raised to 42 °C indicating a temperature-induced increase of the adsorbed amount of SNase. In general, shifting of oscillations of a neutron reflectivity curve to smaller Q-values is a result of an increasing interfacial film thickness. (To be more precise, the width of oscillations in a reflectivity curve, ΔQ, is inversely proportional to the total film thickness at the interface, d: $\Delta Q \approx 2\pi/d$.) Here, the formation of a protein adsorbate on the polyelectrolyte multilayer causes this increase in film thickness. However, protein molecules may also penetrate into the PSS final layer of the polyelectrolyte multilayer. Thus, the neutron reflectivity curves measured in the presence of SNase were analyzed on the basis of the structure models shown in Figs. 1(b) and 1(c).

In the fitting analysis of the measured neutron reflectivity curves in the presence of SNase at pD=4.9 and 7.5, the

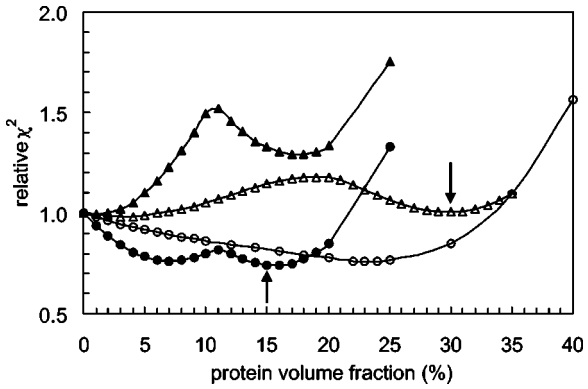

FIG. 4. Quality of the data fitting as a function of the protein volume fraction in the upper 50 Å of the polyelectrolyte multilayer [solid symbols, see Fig. 1(b)] and in the upper 25 Å of the polyelectrolyte multilayer [open symbols, see Fig. 1(c)]. Neutron reflectivity curves at pD=4.9 and 22 °C (solid and open circles) and at pD=7.5 and 22 °C (solid and open triangles) were analyzed. The χ^2-values are normalized to those where no SNase is incorporated into the polyelectrolyte multilayer. Physically reasonable minima are indicated by arrows.

corresponding structure data of the polyelectrolyte multilayers (Table I) were used as fixed parameters. It is noted that this restriction is needed to reduce the number of free fitting parameters. As a consequence, small changes in the polyelectrolyte multilayer structure that might be induced by protein interactions are neglected. The thickness of the protein adsorbate, the protein volume fraction in the adsorbate, and the protein volume fraction in the upper 50 or 25 Å of the polyelectrolyte multilayer were used as fitting parameters [Figs. 1(b) and 1(c)]. The additional roughness parameters in the presence of protein were not found to affect significantly the quality of the data fitting and were thus set to 3 Å. Thus, there are only three free parameters to globally fit a pair of neutron reflectivity curves varying in contrast. Interestingly, it is found that the global χ^2-value according to Eq. (1) is passing through minima as the protein volume fraction in the upper polyelectrolyte multilayer region is increased (Fig. 4). For example, at pD=4.9 and 22 °C, comparable minima at 7% and 15% [50 Å penetration depth, Fig. 1(b)] and at 23% [25 Å penetration depth, Fig. 1(c)] are found. At pD=7.5 and 22 °C, comparable minima are located at 1% [50 Å penetration depth, Fig. 1(b)] and at 3% and 30% [25 Å penetration depth, Fig. 1(c)]. Thus, there is a clear trend that SNase partially penetrates into the upper region of the polyelectrolyte multilayer upon adsorption. It is possible to judge which of these minima represent physically reasonable structures by considering the corresponding data for the thickness of the protein adsorbate on top of the PSS-PAH multilayer and the protein volume fraction within this adsorbate. The thickness of the protein adsorbate should not be drastically smaller than the diameter of SNase which is 45 Å [37] and the protein volume fraction within this adsorbate should not be much larger than about 50% [38]. On the basis of these criteria, one can select the minima marked in Fig. 4 by arrows to deduce the interfacial structures. For comparison, without protein incorporation into the polyelectrolyte multilayer, the SNase adsorbate on top of the multilayer is

TABLE II. Spatial distribution of SNase interacting with an Si-PEI-PSS-(PAH-PSS)$_5$-buffer solution interface.[a]

pD	T (°C)	Model	$\phi_{pro,2}$	$\phi_{pro,3}$	d_3 (Å)
4.9	22	Fig. 1(b)	0.15	0.14	45
4.9	42	Fig. 1(b)	0.23	0.19	48
			$\phi_{pro,3}$	$\phi_{pro,4}$	d_4 (Å)
7.5	22	Fig. 1(c)	0.30	0.29	39
7.5	42	Fig. 1(c)	0.35	0.38	43

[a]For each pD-value, a different Si wafer was used. Interlayer roughnesses are σ_{01}=31 Å, σ_{12}=5 Å, σ_{23}=3 Å, σ_{34}=3 Å, and σ_{45}=3 Å.

characterized by a protein volume fraction of 0.82 (pD=7.5,22 °C) or 0.69 (pD=4.9,22 °C) and a layer thickness of 22 Å (pD=7.5,22 °C) or 14 Å (pD=4.9,22 °C). In a similar way, results were obtained from the measurements performed at 42 °C. It is noted that the quality of the data fitting cannot be improved significantly by choosing a structure model with a larger penetration depth for the protein. In Table II, the spatial distribution of SNase interacting with a PSS-PAH multilayer is summarized for the various conditions studied. For pD=4.9 and D_2O as solvent, calculated neutron reflectivity curves are shown in Fig. 3(b) as solid lines.

Volume fraction profiles for the polyelectrolyte and the protein at pD=4.9 and 7.5 are plotted in Fig. 5. The profiles

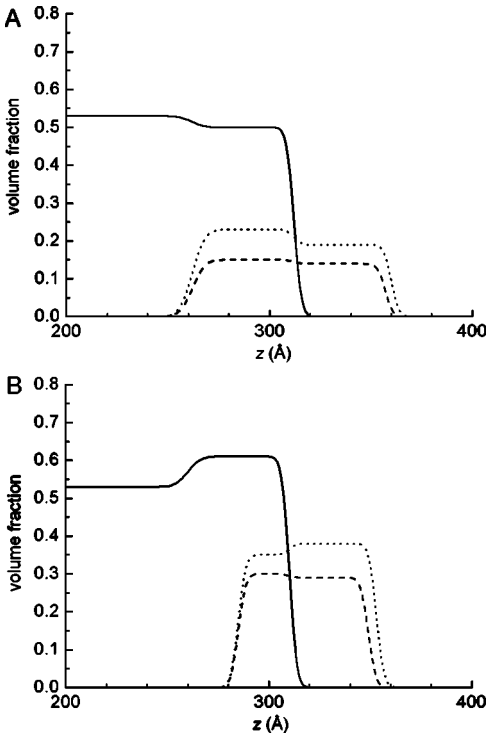

FIG. 5. Volume fraction profiles of a polyelectrolyte multilayer (solid lines), SNase at 22 °C (dashed lines), and SNase at 42 °C (dotted lines). Data are shown at pD=4.9 (A) and pD=7.5 (B). The surface of the silicon wafer is located at z=0.

were calculated from the data listed in Tables I and II. At both *p*D-values, the profiles clearly indicate that SNase penetrates into the polyelectrolyte multilayer upon adsorption. The reason for this behavior may be understood by considering the following findings: With increasing temperature there is an increasing amount of adsorbed SNase at the polyelectrolyte multilayer [Fig. 5(a) and 5(b)]. At $p\mathrm{D}=4.9$, the protein surface concentration is increasing from 1.8 mg m^{-2} at 22 °C to 2.7 mg m^{-2} at 42 °C. At $p\mathrm{D}=7.5$, one calculates 2.5 mg m^{-2} at 22 °C and 3.3 mg m^{-2} at 42 °C (the protein surface concentrations have been calculated by integrating the protein volume fraction profiles). Assuming an equilibrium between dissolved and adsorbed protein molecules, the van't Hoff equation predicts an endothermic adsorption when the degree of adsorption is enhanced by an increase in temperature. Thus, the adsorption of SNase at the polyelectrolyte multilayer will be driven by an increase in entropy. This entropy increase is most likely due to hydrophobic interactions and/or a complexation between the protein molecules and the polyelectrolyte chains. Hydrophobic interactions are likely to be present, since protein molecules display hydrophobic patches at their surface and the polyelectrolytes have hydrophobic chemical groups, especially the PSS. On the other hand, negatively charged PSS chains are binding to the positively charged SNase molecules thereby releasing a corresponding number of monovalent counterions. It is interesting to note that at $p\mathrm{D}=4.9$, SNase is penetrating deeper into the polyelectrolyte multilayer than at $p\mathrm{D}=7.5$ (Fig. 5). Furthermore, at $p\mathrm{D}=4.9$, the temperature-induced mass increase of adsorbed SNase is larger within the upper polyelectrolyte multilayer region than on top of the multilayer [Fig. 5(a)]. Thus, it appears that SNase preferentially penetrates into the polyelectrolyte multilayer at a low *p*D-value where it is highly charged and carries a large number of negatively charged counterions. Therefore, the penetration of SNase into the polyelectrolyte multilayer is likely to be related to a complexation between SNase molecules and PSS chains in addition to hydrophobic interactions.

V. CONCLUSIONS

In this study, we have determined the volume fraction profile of SNase that is adsorbed at a polyelectrolyte multilayer by using neutron reflectometry. The experiments were performed at *p*D-values where SNase carries a net positive charge and interacts with the PSS final layer of the polyelectrolyte multilayer under electrostatic attraction conditions. The analysis of the neutron reflectivity curves indicates that SNase is partially penetrating into the polyelectrolyte multilayer upon adsorption. This penetration is preferred, when the positive charge of the protein is high. It is concluded that under this condition SNase molecules and PSS chains interact by a complexation associated with a release of counterions which represents an entropic driving force for protein adsorption.

ACKNOWLEDGMENTS

We thank the Deutsche Forschungsgemeinschaft (DFG) and the Hahn-Meitner-Institut Berlin for financial support.

[1] *Biopolymers at Interfaces*, edited by M. Malmsten (Marcel Dekker, New York, 2003).
[2] *Proteins at Interfaces II* edited by T. A. Horbett and J. L. Brash (American Chemical Society, Washington, D.C., 1995).
[3] A. Kondo and H. Fukuda, J. Colloid Interface Sci. **198**, 34 (1998).
[4] T. Vermonden, C. A. Giacomelli, and W. Norde, Langmuir **17**, 3734 (2001).
[5] R. J. Marsh, R. A. L. Jones, and M. Sferrazza, Colloids Surf., B **23**, 31 (2002).
[6] C. Czeslik and R. Winter, Phys. Chem. Chem. Phys. **3**, 235 (2001).
[7] C. Czeslik, C. Royer, T. Hazlett, and W. Mantulin, Biophys. J. **84**, 2533 (2003).
[8] A. Wittemann, B. Haupt, and M. Ballauff, Phys. Chem. Chem. Phys. **5**, 1671 (2003).
[9] C. Czeslik, R. Jansen, M. Ballauff, A. Wittemann, C. A. Royer, E. Gratton, and T. Hazlett, Phys. Rev. E **69**, 021401 (2004).
[10] C. Czeslik, G. Jackler, R. Steitz, and H.-H. von Grünberg, J. Phys. Chem. B **108**, 13395 (2004).
[11] A. Wittemann and M. Ballauff, Anal. Chem. **76**, 2813 (2004).
[12] T. Neumann, B. Haupt, and M. Ballauff, Macromol. Biosci. **4**, 13 (2004).
[13] G. Decher, Science **277**, 1232 (1997).
[14] M. Schönhoff, Curr. Opin. Colloid Interface Sci. **8**, 86 (2003).
[15] R. Steitz, V. Leiner, R. Siebrecht, and R. von Klitzing, Colloids Surf., A **163**, 63 (2000).
[16] K. Büscher, K. Graf, H. Ahrens, and C. A. Helm, Langmuir **18**, 3585 (2002).
[17] H. Riegler and F. Essler, Langmuir **18**, 6694 (2002).
[18] P. M. Biesheuvel and M. A. Cohen Stuart, Langmuir **20**, 4764 (2004).
[19] F. Caruso and H. Möhwald, J. Am. Chem. Soc. **121**, 6039 (1999).
[20] F. Caruso and C. Schüler, Langmuir **16**, 9595 (2000).
[21] P. Schwinté, J.-C. Voegel, C. Picart, Y. Haikel, P. Schaaf, and B. Szalontai, J. Phys. Chem. B **105**, 11906 (2001).
[22] P. Schwinté, V. Ball, B. Szalontai, Y. Haikel, J.-C. Voegel, and P. Schaaf, Biomacromolecules **3**, 1135 (2002).
[23] A. P. Ngankam, G. Mao, and P. R. Van Tassel, Langmuir **20**, 3362 (2004).
[24] J. P. Santos, E. R. Welsh, B. P. Gaber, and A. Singh, Langmuir **17**, 5361 (2001).
[25] M. Fang, P. S. Grant, M. J. McShane, G. B. Sukhorukov, V. O. Golub, and Y. M. Lvov, Langmuir **18**, 6338 (2002).
[26] G. Ladam, C. Gergely, B. Senger, G. Decher, J.-C. Voegel, P. Schaaf, and F. J. G. Cuisinier, Biomacromolecules **1**, 674 (2000).
[27] G. Ladam, P. Schaaf, F. J. G. Cuisinier, G. Decher, and J.-C.

Voegel, Langmuir **17**, 878 (2001).
[28] V. Ball, M. Winterhalter, P. Schwinté, P. Lavalle, J.-C. Voegel, and P. Schaaf, J. Phys. Chem. B **106**, 2357 (2002).
[29] C. Picart, K. Sengupta, J. Schilling, G. Maurstad, G. Ladam, A. R. Bausch, and E. Sackmann, J. Phys. Chem. B **108**, 7196 (2004).
[30] T. P. Russell, Mater. Sci. Rep. **5**, 171 (1990).
[31] H. Seemann, R. Winter, and C. A. Royer, J. Mol. Biol. **307**, 1091 (2001).
[32] F. Mezei, R. Golub, F. Klose, and H. Toews, Physica B **213/214**, 898 (1995).
[33] W. N. Hansen, J. Opt. Soc. Am. **58**, 380 (1968).
[34] www.ncnr.nist.gov/resources/n-lengths/list.html.
[35] T. V. Chalikian, M. Totrov, R. Abagyan, and K. J. Breslauer, J. Mol. Biol. **260**, 588 (1996).
[36] I. Estrela-Lopis, S. Leporatti, S. Moya, A. Brandt, E. Donath, and H. Möhwald, Langmuir **18**, 7861 (2002).
[37] G. Panick, R. Malessa, R. Winter, G. Rapp, K. J. Frye, and C. A. Royer, J. Mol. Biol. **275**, 389 (1998).
[38] G. Jackler, R. Steitz, and C. Czeslik, Langmuir **18**, 6565 (2002).